

# Comparison of C–Cl and Si–Cl Bonds. A Valence Bond Study

David Lauvergnat,<sup>†</sup> Philippe C. Hiberty,<sup>\*,†</sup> David Danovich,<sup>‡</sup> and Sason Shaik<sup>\*,‡</sup>

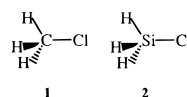
The Laboratoire de Chimie Théorique, Université de Paris-Sud, 91405 Orsay Cedex, France, and  
The Department of Organic Chemistry, The Hebrew University, 91904 Jerusalem, Israel

Received: January 10, 1996<sup>⊗</sup>

VB calculations with breathing orbitals (BOVB) show that the  $\text{H}_3\text{Si}-\text{Cl}$  and  $\text{H}_3\text{C}-\text{Cl}$  bonds are qualitatively different. The differences are rooted in the properties of the  $\text{H}_3\text{Si}^+$  and  $\text{H}_3\text{C}^+$  species. Thus, the  $\text{H}_3\text{C}^+$  cation has an evenly distributed charge and relatively large ionic radius, and therefore the cation maintains a long distance from the counterion  $\text{Cl}^-$ . Consequently, the ionic–covalent mixing remains of secondary influence and shortens slightly the  $R_{\text{CCl}}$  distance in agreement with the Pauling recipe for polar bonds. On the other hand, in  $\text{H}_3\text{Si}^+$  the charge is highly localized on silicon. Consequently, the cation acquires a diminished effective size along the missing coordination site. This allows a close approach of  $\text{Cl}^-$  as well as a very large electrostatic interaction between the  $\text{Si}^+$  and  $\text{Cl}^-$  centers in the ionic VB structure. Consequently, the ionic potential energy curve  $R_3\text{Si}^+\text{Cl}^-$  approaches the corresponding covalent curve to a near-degeneracy. The ensuing VB mixing renders the Si–Cl bond a *true charge-shift bond whose major character is the charge fluctuation inherent in the resonating wave function*. The effect of ionicity on the Si–Cl bond length does not follow the Pauling recipe. Indeed, by mixing of the ionic structure the  $R_{\text{SiCl}}$  minimum shifts to a longer distance in comparison with the covalent minimum. The new minimum is simply an intermediate distance between the covalent and ionic minima in keeping with the charge-shift nature of the bond. The manifestations of the diminished effective size of  $R_3\text{Si}^+$  are its strong coordinating ability with electronegative and electron-rich ligands. Implications on the  $R_3\text{Si}^+$  problem are discussed.

## Introduction

Bonding in first vs higher row atoms poses quite a few interesting problems. The bond strength issue is itself intriguing. Thus, while the Si–X bonds are significantly weaker than their C–X analogs for X = H, C, S, the reverse is true for X = F, Cl, Br, I, O, etc.<sup>1,2a</sup> This trend is general and applies to N–X vs P–X bonds, as well as to bonds of higher rows, e.g., Sn–X and Ge–X vs C–X.<sup>1a,b</sup> Another puzzling feature is the reluctance of  $R_3\text{Si}-\text{X}$  bond to heterolyze<sup>2–6</sup> in solution, in comparison with the ease of heterolysis in  $R_3\text{C}-\text{X}$  compounds. So rare are the  $R_3\text{Si}^+\text{X}^-$  species in condensed phase that a compound like  $\text{Ph}_3\text{SiClO}_4$  that appears initially as an excellent candidate for an ionic bond was found to be a covalent solid exhibiting a Si–O bond.<sup>7</sup> In contrast, the carbon analog is definitely ionic,  $\text{Ph}_3\text{C}^+\text{ClO}_4^-$ .<sup>8</sup> This intriguing feature is connected with the continuous search for  $R_3\text{Si}^+\text{X}^-$  in condensed phases<sup>2,9–17</sup> and with the recent controversies surrounding the findings and their interpretations.<sup>6,12–17</sup> In the course of the search it has become apparent that Si has a very strong affinity for covalent interactions, much stronger indeed than carbon, and that it takes counterions such as hexabromocarborene to approach, albeit not completely, an ion pair;  $R_3\text{Si}^+\text{X}^-$ .<sup>10</sup> These differences between bonding in second-row and first-row atoms are truly fundamental and require understanding. However, before these issues can be properly addressed, a prerequisite step must be taken: understanding of the nature of the bonds. The present paper deals with this initial step by investigating the C–Cl and Si–Cl bonds in the simplest model compounds **1** and **2**.



The investigation is carried out by means of valence bond (VB) calculations, based on the recently developed VB method, that utilizes orbitals which are adapted to the charge fluctuation inherent in the bonding, the so-called breathing-orbital VB (BOVB) method.<sup>18,19</sup> The BOVB method takes into account part of the dynamic correlation and is suited particularly to bonding situations which involve considerable covalency–ionicity fluctuations, as C–Cl and Si–Cl. Based on the BOVB method we report bonding energies and ionic–covalent resonance energies, and we attempt to trace the origins of the reluctance of Si–Cl to ionize in terms of fundamental properties of its constituent fragments. As shall be seen, the origins of the higher strength of Si–Cl vs C–Cl, its excess ionic character, and at the same time its higher ionic–covalent resonance energies *can all be traced to the effectively smaller  $\text{H}_3\text{Si}^+$  ionic radius, compared with  $\text{H}_3\text{C}^+$ , along the missing coordination site*.

## Theoretical Methods

All calculations used the 6-31G\* basis set. The VB calculations were carried out with the Utrecht package TURTLE.<sup>20</sup> This is a general nonorthogonal CI program which performs linear variation as well as orbital optimization simultaneously on a given set of VB configurations. The orbital optimization is based on the super-CI technique<sup>21</sup> related to the generalized Brillouin theorem.<sup>22</sup> The VB potential energy curves (Figures 1 and 2) were traced by performing the VB calculations of the individual configurations and of the final state on geometries

<sup>†</sup> Laboratoire de Chimie Théorique, associated with the CNRS, UA 506.

<sup>‡</sup> Hebrew University.

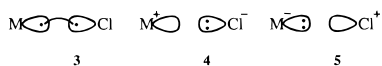
<sup>⊗</sup> Abstract published in *Advance ACS Abstracts*, March 1, 1996.

determined at the GVB (1/2) level, i.e., with local correlation of the electron pair of the M–Cl bond in the framework of the generalized valence bond method.<sup>23</sup> These geometries correspond to a preoptimization of all the geometric parameters of H<sub>3</sub>MCl (M = C, Si) at different  $R_{\text{MCl}}$  distances taken as the principal coordinate in Figures 1 and 2.

An important feature of our VB calculations is that all the orbitals that are used are strictly localized on a single fragment, MH<sub>3</sub> or Cl, so as to ensure a clear correspondence between the mathematical expressions of the VB structures and their physical meaning, ionic or covalent. Among the electrons and orbitals, one distinguishes an active space, made of the orbitals and the electrons that are directly involved in the bond breaking, from an inactive space where the orbitals keep the same occupancy throughout the M–Cl coordinate. The active space is treated at the VB level and its electrons are explicitly correlated, while the inactive part of the molecule is described as a set of doubly occupied orbitals, so that the correlation of inactive electrons is not explicitly taken into account. The frozen core approximation has been used in all calculations, i.e., the core orbitals (1s for carbon, 1s, 2s, and 2p for silicon and chlorine) are not optimized in the VB calculations but arise from calculations of the H<sub>3</sub>M and Cl fragments at the restricted open-shell Hartree–Fock level (ROHF)<sup>24</sup> level.

The basis set that we use, 6-31G\*, is small and therefore the BOVB method is expected to provide a modest accuracy of the order of  $\pm 10\%$ . The BOVB method has been shown to reproduce the dissociation energy curve of another polar molecule, HF, with an accuracy of about 2 kcal/mol relative to the full CI curve, in 6-31G\*\* basis set. Yet the full CI itself underestimates the bonding energy by 5 kcal/mol, and this is an indication that larger basis sets are needed for polar molecules. Since chlorine is more polarizable than fluorine, the need for polarization functions higher than d can be anticipated for both Si–Cl and C–Cl bonds, to better account for angular electronic correlation in the ionic VB structures. Very accurate dissociation energy curves would therefore require larger basis sets, but also additional VB structures to take angular correlation into account. While this can certainly be done within the BOVB method, this will also result in a more complicated wave function and less clearly defined individual VB structures. Thus, the definition of ionic or covalent structures rests on the concept of localization of the electrons, and this meaning is largely lost if basis sets involving very diffuse or high-rank polarization wave functions are used. It was therefore decided to sacrifice some of the accuracy and gain the conceptual advantage of a physically lucid wave function, by keeping the BOVB method in its simple form with a basis set of moderate size.

**VB and BOVB Calculations of H<sub>3</sub>M–Cl.** Three VB configurations, 3–5, are needed to describe the M–Cl bond pair.



The first configuration, 3, is the covalent Heitler–London ( $\Psi_{\text{HL}}$ ) structure, while the other two are the ionic structures. The ground state wave function at any distance along the  $R_{\text{MCl}}$  coordinate is given by a linear combination of the three structures:

$$\Psi_{\text{M-Cl}} = C_1 \Psi_{\text{M-}\cdots\text{Cl}} + C_2 \Psi_{\text{M}^+\text{Cl}^-} + C_3 \Psi_{\text{M}^-\text{Cl}^+} \quad (1)$$

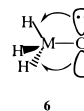
The VB wave function  $\Psi_{\text{M-Cl}}$  in (1) is obtained by simultaneously optimizing both the coefficients of the determinants as well as all their orbitals for self-consistency, so as to minimize

the ground state energy. At the simplest VB level, the three VB structures 3–5 are defined based on a common set of orbitals and differ from each other by their orbital occupancies. These orbitals correspond therefore to a mean-field approximation because they are not allowed to adapt freely to the local fields of the individual configurations. We refer to this level as simply VB.

A more accurate wave function, yielding much better dissociation energies, can be obtained by allowing all the orbitals to optimize freely, so that each VB structure ends up having its specific set of orbitals, different from one VB structure to the other. Thus, the orbitals are well adapted, in each configuration, to the local fields created by the fragments that can in turn be either neutral or ionic. One can also view the orbitals optimized in such a way as following the fluctuation of the bonding electrons from one center to the other by instantaneously rearranging in size and shape (this is the origin of the names “breathing orbitals” (BO) and the associated BOVB method).

Several levels of sophistication are possible within the BOVB framework.<sup>18b</sup> Thus, the active electrons in an ionic structure can either be located in the same doubly occupied orbital or in a pair of split singly occupied orbitals much like in GVB theory.<sup>23</sup> This latter option has been chosen in the present work in order to better describe the ionic structures by taking some radial electron correlation into account. We refer to this level as BOVB(I).

At the BOVB(II) level we take into account also the hyperconjugative interactions between the lone pairs and the  $\sigma_{\text{MH}}^*$  orbitals, 6. This is done by adopting the delocalized forms



of the respective inactive doubly occupied orbitals. The hyperconjugative interactions differ for the three individual configurations and therefore the BOVB(II) level allows us to compute the effects of  $\pi$ -bonding which is often considered to be important in Si–X bonds.<sup>25</sup>

The importance of each VB structure as a contributor to the ground state can be appreciated by considering the coefficients in eq 1, or more meaningfully by calculating the weights of each VB structures by means of the Chirgwin–Coulson formula:<sup>26</sup>

$$W_n = C_n^2 + \sum_{m \neq n} C_m C_n S_{mn} \quad (2)$$

Here  $W_n$  is the weight of the VB structure  $n$ ,  $C_n$  its coefficient, and  $S_{mn}$  the overlap between VB structures  $m$  and  $n$ .

Net atomic charges for  $\text{R}_3\text{M}^+$  cations (R = H, CH<sub>3</sub>; M = C, Si) were calculated by means of the natural bond orbital (NBO) analysis<sup>27</sup> at the Hartree–Fock level. These calculations were performed with the GAUSSIAN-92 package<sup>28</sup> of programs.

## Results and Discussion

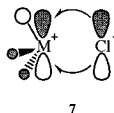
Table 1 shows the bond energies calculated at the various VB levels. It is apparent that the VB method reproduces the relative order of the two bond strengths at all the levels. However, it is seen that the breathing orbital effect is decisive for quantitative accuracy. Thus, the adaptation of the active orbitals to the charge fluctuation inherent in the two-electron bond constitution is a physical effect that must be properly taken into account. Another interesting trend in the table is the effect of  $\pi$ -bonding in the two compounds. Comparing BOVB(I) to BOVB(II)

**TABLE 1: Bond Energies  $D_e$  (kcal/mol) for  $\text{H}_3\text{C}-\text{Cl}$  and  $\text{H}_3\text{Si}-\text{Cl}$  at Various Levels**

species	exptl <sup>a</sup>	VB <sup>b</sup>	BOVB(I) <sup>b</sup>	BOVB(II) <sup>b</sup>	G1 <sup>c</sup>	G2 <sup>c</sup>
$\text{H}_3\text{CCl}$	87.3	61.1	72.8	79.9	88.9	88.3
$\text{H}_3\text{SiCl}$	110.7	79.2	91.2	101.7	111.9	110.7

<sup>a</sup>  $D_e$  obtained from experimental  $D_0$  values quoted in ref 29b and corrected by a calculated  $\Delta\text{ZPE}$  (ref 29a). <sup>b</sup> Optimized geometric values (GVVB(1/2)/6-31G\*) are,  $R_{\text{CCl}} = 1.815 \text{ \AA}$ ;  $R_{\text{CH}} = 1.078 \text{ \AA}$ ;  $\theta(\text{HCCl}) = 108.1^\circ$ ;  $R_{\text{SiCl}} = 2.086 \text{ \AA}$ ;  $R_{\text{SiH}} = 1.468 \text{ \AA}$ ;  $\theta(\text{HSiCl}) = 108.3^\circ$ . <sup>c</sup> G1 and G2 values from ref 29.

shows that the  $\pi$ -bonding is significant in both compounds, 7.1 and 10.5 kcal/mol, respectively, for  $\text{CH}_3\text{Cl}$  and  $\text{SiH}_3\text{Cl}$ . A detailed analysis of the effect in the three configurations shows that the ionic structure, **2**, exhibits the largest effect (9.5 and 14.9 kcal/mol, respectively), allowing the lone pairs of the  $\text{Cl}^-$  donor to back-donate some electron density into the  $\pi^*$  type of orbitals of  $\text{MH}_3^+$  as in **7**. Nevertheless, the covalent HL

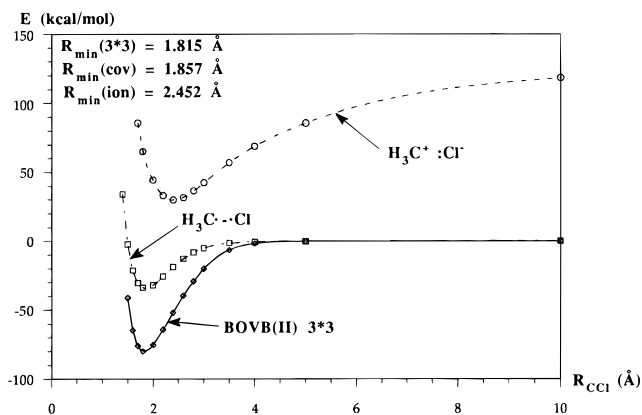
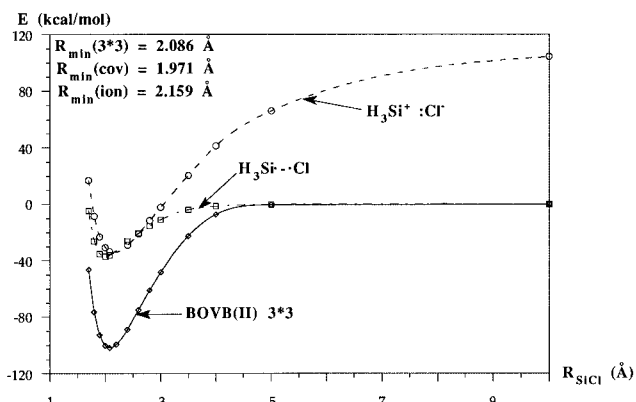


configuration also exhibits  $\pi$ -bonding, albeit smaller than in the ionic structure. This latter effect is almost the same for C and Si being 6.4 and 7.3 kcal/mol, respectively. The significant  $\pi$ -bonding effect in the HL configuration indicates that part of the  $\pi$ -bonding in the final state should be attributed to the tendency of the fragments to minimize their four-electron repulsive interactions by partial delocalization. The final  $\pi$ -bonding is an average of the contributions due to the ionic and the HL structures, according to the contribution to the bond wave function in eq 1.

Finally, our BOVB(II) results can be compared to the results obtained by the G1 and G2 methods<sup>29</sup> and to the experimental results. It is apparent that the accuracy of the BOVB(II) method is less than the very accurate G2 method and yields bonding energies which are too small by 7.4 and 9.4 kcal/mol, respectively, for the C–Cl and Si–Cl bonds, and bond lengths 0.034 and 0.037  $\text{\AA}$  too long relative to experiment.<sup>30</sup> This rather modest performance must be assessed by keeping in mind that the G2 method uses much larger basis sets than 6-31G\* which was selected for the BOVB study. Thus, since the accuracy of the BOVB results is still reasonable (8.5–9.0%), the gain of insight should balance this modest deficiency and favors to keep the small basis set (see discussion in the Theoretical Methods section).

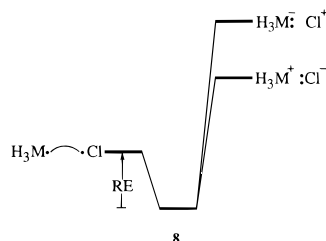
Figures 1 and 2 show the VB energy curves for  $\text{CH}_3\text{Cl}$  and  $\text{SiH}_3\text{Cl}$ , at the BOVB(II) level. The curves are traced from 1.6 to 10  $\text{\AA}$ . At each point we present the two lowest VB structures, as well as the complete adiabatic state energy curve, marked as BOVB(II) 3\*3.

It is seen that in both molecules, the HL configuration is bonded relative to the separated fragments by a significant amount. This bonding energy is the covalent contribution that arises solely from the spin pairing of the two electrons which are, in turn, localized on their respective fragments.<sup>31,32</sup> These covalent bond energies are ca. 34 kcal/mol for  $\text{CH}_3\text{Cl}$  and 37 kcal/mol for  $\text{SiH}_3\text{Cl}$ . It is apparent therefore that the interaction between the HL and the ionic configurations is very important for both bonds and it shifts the minimum of the respective states away from the minima of the HL configurations. In the case of  $\text{CH}_3\text{Cl}$  this shift is from 1.857 to 1.815  $\text{\AA}$  which is relatively small and follows the normal tendency expected from polar bonds, namely C–Cl bond shortening.<sup>1b</sup> In contrast, in the case

**Figure 1.**  $\text{H}_3\text{C}-\text{Cl}$  dissociation energy curves for the pure ionic ( $\text{H}_3\text{C}^+\text{Cl}^-$ ), the pure covalent ( $\text{H}_3\text{C}-\text{Cl}$ ), and the full state for the C–Cl bond (BOVB(II) 3\*3).**Figure 2.**  $\text{H}_3\text{Si}-\text{Cl}$  dissociation energy curves for the pure ionic ( $\text{H}_3\text{Si}^+\text{Cl}^-$ ), the pure covalent ( $\text{H}_3\text{Si}-\text{Cl}$ ), and the full state for the Si–Cl bond (BOVB(II) 3\*3).

of  $\text{SiH}_3\text{Cl}$  the shift is both significant, from 1.971 to 2.086  $\text{\AA}$ , as well as operating precisely in an opposite direction to the common effect predicted for polar bonds.<sup>1b</sup> It is clear therefore that, while the charge-shift resonance energy<sup>32</sup> due to ionic–covalent mixing is crucial in both bonds, still the two bonds behave in a qualitatively different manner in their response to the charge fluctuation.

The formation of the ground state bond at each point of the  $R_{\text{M}\cdots\text{Cl}}$  coordinate can be conceptualized in terms of the VB mixing diagram,<sup>31,32</sup> in **8**. Thus, the covalent VB structure mixes



primarily with the lowest ionic structure, through an interaction matrix element which is nothing but the classical resonance integral  $\beta$ . There results an increase of the bond energy, relative to the covalent curve, by a quantity RE which is the resonance energy due to charge shift (or charge fluctuation) and which obeys the qualitative rules of perturbation theory: the more negative the  $\beta$  integral and/or the smaller the covalent–ionic energy gap, the larger the resonance energy.

The variation of the resonance integral  $\beta$  as a function of the interatomic distance is plotted in Figure 3 for the C–Cl and

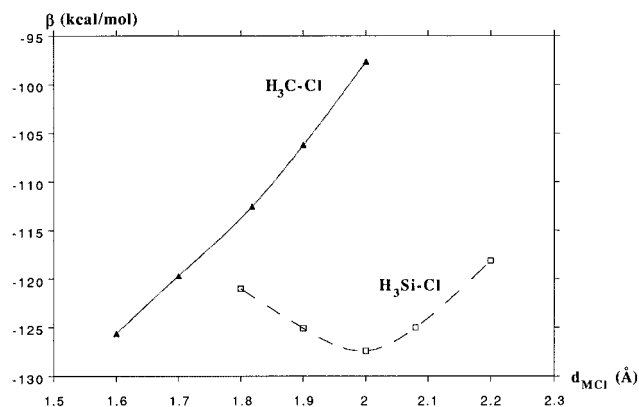


**Figure 3.** Variation of the  $\beta$  resonance integral in the  $\text{H}_3\text{C}-\text{Cl}$  and  $\text{H}_3\text{Si}-\text{Cl}$  cases, as a function of the  $\text{M}-\text{Cl}$  distance ( $\text{M} = \text{C}, \text{Si}$ ).

**TABLE 2: Weights and Coefficients of Covalent and Ionic Structures for  $\text{H}_3\text{C}-\text{Cl}$  and  $\text{H}_3\text{Si}-\text{Cl}$  at Various Levels**

	coefficients		weights	
	BOVB(I)	BOVB(II)	BOVB(I)	BOVB(II)
$\text{H}_3\text{C}^{\bullet}-\text{Cl}$	0.652	0.646	0.622	0.616
$\text{H}_3\text{C}^+\text{Cl}^-$	0.351	0.358	0.262	0.269
$\text{H}_3\text{C}^-\text{Cl}^+$	0.191	0.190	0.116	0.115
$\text{H}_3\text{Si}^{\bullet}-\text{Cl}$	0.648	0.628	0.594	0.572
$\text{H}_3\text{Si}^+\text{Cl}^-$	0.501	0.522	0.436	0.459
$\text{H}_3\text{Si}^-\text{Cl}^+$	0.076	0.075	-0.030	-0.031

$\text{Si}-\text{Cl}$  bonds. In the first case,  $\beta$  becomes increasingly more negative as the interatomic distance decreases from the covalent minimum, while at the same time the covalent-ionic energy gap remains relatively constant (see Figure 1). This explains why the ground state minimum is shorter than the covalent minimum. On the other hand, in the  $\text{Si}-\text{Cl}$  bond the  $\beta$  integral reaches a maximum negative value between the covalent and ionic minima (ca. 2 Å). This, added to the near-degeneracy of the covalent and ionic curves, is the reason why the resonance energy peaks in this region of the potential surface, thus imposing a final bond distance that is an average between the minima of the covalent and ionic VB structures.

The coefficients of the covalent and ionic structures in the ground states of  $\text{H}_3\text{SiCl}$  and  $\text{H}_3\text{CCl}$  are displayed in Table 2, along with their calculated weights. At the BOVB(II) level, it appears that the  $\text{C}-\text{Cl}$  bond is mostly covalent, with a weight of ca. 62%, as compared with a weight of 27% for the lowest ionic structure,  $\text{C}^+\text{Cl}^-$ , while the other ionic structure is marginal. On the other hand, the  $\text{Si}-\text{Cl}$  bond has rather similar covalent and ionic weights (respectively 57 and 46%), in agreement with the near degeneracy of the corresponding VB structures, at equilibrium bonding distance. The highest ionic VB structure,  $\text{Si}^-\text{Cl}^+$ , is totally negligible and even comes out with a negative weight, which in the Chirgwin-Coulson definition is interpreted as close to zero.

As may be seen from Figures 1 and 2, the resonance energy RE is strikingly large, ca. 46 kcal/mol for  $\text{CH}_3\text{Cl}$  and ca. 66 kcal/mol for  $\text{SiH}_3\text{Cl}$ . In fact, in both cases the major bonding interaction that glues the two fragments is the charge shift resonance energy, and for the  $\text{Si}-\text{Cl}$  bond this contribution is truly dominant being  $\approx 65\%$  of the total bond energy. Two factors join to make the RE more dominant in the  $\text{SiH}_3\text{Cl}$  case in comparison with  $\text{CH}_3\text{Cl}$ . The first is the configuration energy gap between the HL and the major ionic structure  $\text{MH}_3^+\text{Cl}^-$ , in **8**, and the second is their interaction matrix element. Since the BOVB(II) calculations show that the effective matrix element is approximately the same for the two molecules (Figure 3), we focus only on the energy gap factor.

**TABLE 3: Covalent and Ionic Radii<sup>a</sup> of  $\text{SiH}_3$  and  $\text{CH}_3$**

species	$r$ (Å)
$\text{SiH}_3$	0.981
$\text{CH}_3$	0.867
$\text{SiH}_3^+$	0.349
$\text{CH}_3^+$	0.642

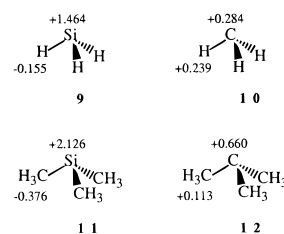
<sup>a</sup>  $r_{\text{Cl}} = 0.99$  Å;  $r_{\text{Cl}^-} = 1.81$  Å; from ref 1b.

At the asymptote of the potential energy curves at 10 Å the energy gap for  $\text{SiH}_3\text{Cl}$  is ca. 11 kcal/mol smaller than the corresponding gap for  $\text{CH}_3\text{Cl}$ , owing to the greater electronegativity of carbon relative to silicon. While this would account for some of the difference of the corresponding RE's, it is clearly insufficient. The more spectacular effect seems to be the behavior of the ionic curves. Thus, it can be seen that the  $\text{H}_3\text{C}^+\text{Cl}^-$  curve has a minimum at 2.452 Å and its energy well is 89.1 kcal/mol deep relative to 10 Å. In contrast, the  $\text{H}_3\text{Si}^+\text{Cl}^-$  curve in Figure 2 has a minimum at 2.159 Å and an energy well of ca. 139 kcal/mol relative to 10 Å. Moreover, the ionic minimum of  $\text{H}_3\text{Si}^+\text{Cl}^-$  coincides almost with the corresponding HL minimum, in contrast with  $\text{H}_3\text{C}^+\text{Cl}^-$  whose minimum is displaced by ca. 0.6 Å to a longer distance relative to the corresponding HL minimum. Consequently, the configuration energy gap in the  $\text{H}_3\text{SiCl}$  case collapses to almost zero near the HL minimum followed by a major charge-shift RE due to the configuration mixing. In fact, the  $\text{H}_3\text{Si}-\text{Cl}$  bond may well be described by a resonating wave function, eq 3, unlike the  $\text{H}_3\text{C}-$

$$\Psi_{\text{H}_3\text{SiCl}} = N[\Psi_{\text{HL}} + \Psi_{\text{H}_3\text{Si}^+\text{Cl}^-}] \quad (3)$$

$\text{Cl}$  bond which remains mostly covalent despite of its significant RE. This behavior of the ionic VB structure is important and merits further elucidation. How is it that the ionic minimum for  $\text{H}_3\text{Si}^+\text{Cl}^-$  is shorter than the minimum for  $\text{H}_3\text{C}^+\text{Cl}^-$ ?

To understand this counterintuitive effect we calculated the charge distributions of a few  $\text{R}_3\text{M}^+$  fragments which are shown in **9–12**, calculated at the same Hartree-Fock-optimized ge-

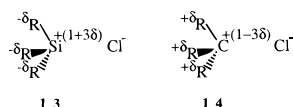


ometries they possess at the respective  $\text{R}_3\text{M}-\text{Cl}$  molecules. Thus, it is seen that the positive charge in  $\text{R}_3\text{Si}^+$  is virtually located on the Si, while in  $\text{R}_3\text{C}^+$  the charge is dispersed and there remains a very small charge on the central carbon. It is apparent therefore that  $\text{R}_3\text{Si}^+\text{Cl}^-$  will maintain much stronger electrostatic interactions than the corresponding  $\text{R}_3\text{C}^+\text{Cl}^-$  species. This is the reason why the minimum of the latter potential energy curve (Figure 1) is ca. 49 kcal/mol less deep and is displaced to a longer distance in comparison with the  $\text{R}_3\text{Si}^+\text{Cl}^-$  curve (Figure 2).

The BOVB calculations allow us in fact to quantify the effective pure covalent and ionic radii of the  $\text{SiH}_3$  and  $\text{CH}_3$  fragments using the corresponding Cl radii as known quantities. The resulting data are given in Table 3. It is apparent that the pure covalent radii of  $\text{SiH}_3$  and  $\text{CH}_3$  behave as expected, that of  $\text{SiH}_3$  being larger. In contrast, the ionic radii behave opposite to the expectations based on the consideration of atomic size; the  $\text{SiH}_3^+$  is significantly smaller than  $\text{CH}_3^+$ . Based on the charge distribution patterns in **9–12** it is apparent that the

effective size of  $\text{SiH}_3^+$  is reduced significantly along the missing coordination site, by the very large positive charge on Si. This property is more likely accentuated in the trimethylsilyl cation  $(\text{CH}_3)_3\text{Si}^+$ , since as seen in **11**, the net positive charge on the silicon atom is significantly larger than in  $\text{SiH}_3^+$ , **9**. This will make the  $\text{R}_3\text{Si}^+$  cation, in general, an extremely efficient coordinating species for electronegative and electron-rich ligands. Thus, in any condensed phase, the diminished size of  $\text{R}_3\text{Si}^+$  along its missing coordinating site will allow a close approach of ligands (L) with electron pairs of  $\pi$ -electrons. At this short distance, there will always exist a very large charge-shift resonance energy that will stabilize the  $\text{R}_3\text{Si}^+\cdots\text{L}$  species due to significant mixing with the HL structure,  $\text{R}_3\text{Si}^+\cdots\text{L}^+$ . The experimental finding<sup>2–4,6–15,17</sup> and the theoretical analyses,<sup>5,16</sup> as well as the gas phase ligand binding energies of  $\text{R}_3\text{Si}^+$  relative to  $\text{R}_3\text{C}^+$ <sup>1a,e,16</sup> seem to support the above interpretation that  $\text{R}_3\text{Si}^+$  cannot be “freed” due to the close distance approach which is afforded along its missing coordination site.

Another interesting feature of the  $\text{R}_3\text{Si}^+$  fragment in comparison with  $\text{R}_3\text{C}^+$  is apparent from **11** vs **12**. It is seen that in  $\text{R}_3\text{Si}^+$  the R substituents possess a negative charge, while in  $\text{R}_3\text{C}^+$  the positive charge is distributed over all the groups. Thus, the  $\text{R}_3\text{Si}^+\text{Cl}^-$  and  $\text{R}_3\text{C}^+\text{Cl}^-$  ion pairs must possess distinctly different charge distributions, **13** and **14**. Clearly, in **13** the local



R–Si dipoles oppose the local Si–Cl dipole, and consequently the net dipole moment of the ionic structure for  $\text{R}_3\text{SiCl}$  should be quite small in the vicinity of the equilibrium distance. This has been verified by our VB calculations which show that the dipole moment of the ionic structure in the range of 1.9–2.5 Å is  $\approx 2$ –2.5 D, way below the expected  $\approx 8.8$ –12 D for a point charge model at this range of distances. With such a small dipole moment, the ionic structure will be only slightly stabilized by a polar solvent. This slight stabilization will in fact make the ionic and HL configurations, in Figure 2 and in analogous cases, literally degenerate. The result would be again a very large resonance energy which will keep the bond intact.

While this problem must await a proper solvation treatment, it is likely that the root cause for the rare heterolytic activity of the Si–X bond in solution<sup>2</sup> and the rarity of “free”  $\text{R}_3\text{Si}^+$  in comparison with the apparent ubiquity of  $\text{R}_3\text{C}^+$  can be traced to one fundamental property of  $\text{R}_3\text{Si}^+$  cations: *the charge localization on the Si atom, which creates a privileged direction with a small effective size along the missing coordination site*. On the one hand, this property is manifested as a large ionic–covalent resonance energy that is responsible for the higher strength of the Si–X bond as compared with the C–X bond. On the other hand, the same property is manifested in a highly positive Si atom surrounded by neutral or negatively charged alkyl groups (**13**) which inhibit the solvation of a separated  $\text{R}_3\text{Si}^+\text{X}^-$  ion pair. Another possible manifestation of the diminished size of  $\text{R}_3\text{Si}^+$  may well be the known propensity for pentacoordination.<sup>3</sup> As has been shown by us, the pentacoordinated species, which displays a bipyramidal structure, is dominated<sup>33</sup> by the fully ionic VB structure  $\text{X}^-\text{R}_3\text{Si}^+\text{X}^-$  which is strongly stabilized by charge shift resonance.<sup>33</sup> Thus, the small effective size of  $\text{SiR}_3^+$ , in the privileged directions along the axis perpendicular to the plane of the R substituents, would both prohibit heterolysis of the  $\text{R}_3\text{Si}^+\text{X}$  bond and at the same time stabilize a pentacoordinate species. Both effects will contribute to the elusiveness of free persistent  $\text{SiR}_3^+$  cations in

solution. Thus, as a whole, despite the strong charge polarization in the Si–X bond,<sup>34</sup> the small effective size of the cation will tend to make ionic  $\text{R}_3\text{Si}^+\text{X}^-$  chemistry quite rare, as opposed to the ubiquity of this chemistry in the  $\text{R}_3\text{C}^+\text{X}^-$  compounds.<sup>35</sup>

## Conclusion

The pure covalent and pure ionic dissociation energy curves, as well as the state curves resulting from the ionic–covalent mixing have been computed for the  $\text{H}_3\text{C}^+\text{Cl}^-$  and  $\text{H}_3\text{Si}^+\text{Cl}^-$  bonds. In both systems, the purely covalent interactions contribute to the bonding energy approximately the same quantity, 34–37 kcal/mol. In contrast, the ionic interactions are distinctly different, and the difference is rooted in the properties of the  $\text{R}_3\text{Si}^+$  and  $\text{R}_3\text{C}^+$  species. The  $\text{R}_3\text{C}^+$  ion has a delocalized charge distribution, and hence its effective size is large, offering no preferred direction of approach to the counterion  $\text{Cl}^-$ . The result is a diminished electrostatic interaction in the  $\text{R}_3\text{C}^+\text{Cl}^-$  structure and a relatively long C–Cl distance. The mixing of this structure into the covalent HL structure (**3**) shortens slightly the  $R_{\text{CCl}}$  distance and remains of secondary influence, even though the resonance energy (RE) due to mixing is significant. In contrast, in  $\text{R}_3\text{Si}^+$  the positive charge is localized on the silicon atom, which thereby acquires a diminished effective size along the missing coordination site. This allows a close approach of the  $\text{Cl}^-$  to  $\text{R}_3\text{Si}^+$  in the ionic structure and therefore a very large electrostatic interaction ensues. The ionic energy curve  $\text{R}_3\text{Si}^+\text{Cl}^-$  approaches therefore the covalent HL curve to a near degeneracy leading thereby to a large covalent–ionic resonance energy which is responsible for more than half of the Si–Cl bond energy.

Another difference between the C–Cl and Si–Cl bonds is the behavior of the resonance integrals,  $\beta(\text{C}^+\text{Cl}^-)$  and  $\beta(\text{Si}^+\text{Cl}^-)$ , that couple the chlorine atom respectively to methyl and silyl, as a function of the bonding distance  $R$ . The  $|\beta(\text{C}^+\text{Cl}^-)|$  quantity increases (in absolute magnitude) as  $R$  decreases, resulting in a C–Cl distance shorter than the covalent minimum. In contrast,  $|\beta(\text{Si}^+\text{Cl}^-)|$  peaks between the covalent and ionic minima in the Si–Cl case. This results in an equilibrium Si–Cl bond length intermediate between the covalent and ionic minima.

Solvent effects are not expected to change drastically the  $\text{H}_3\text{Si}^+\text{Cl}^-$  bonding picture, which can be generalized to  $\text{R}_3\text{Si}^+\text{Cl}^-$  bonds. The reason why this latter system does not appear to solvolyze via free ions may be attributed, on the one hand, to the loss of the larger ionic–covalent resonance energy which necessarily attends a heterolytic process, and on the other hand to the lack of available direction of approach for the solvent to stabilize the  $\text{R}_3\text{Si}^+\text{X}^-$  separated ion pair. To investigate these problems in a rigorous manner, a VB treatment explicitly including solvent effects is currently in progress in our laboratories.

**Acknowledgment.** The research at the Hebrew University is supported by the ISF, administered by the Israeli Academy of Sciences and Humanities. We are grateful to J. H. van Lenthe and C. P. Byrman for making their TURTLE valence bond program available to us.

## References and Notes

- (1) (a) Leroy, G.; Temsamani, D. R.; Wilante, C. *J. Mol. Struct. (THEOCHEM)* **1994**, 306, 21. (b) Pauling, L. In *The Nature of the Chemical Bond*; 3rd ed; Cornell University, 1960. (c) Shin, S. K.; Beauchamp, J. L. *J. Am. Chem. Soc.* **1989**, 111, 900. (d) Jasinski, J. M.; Becerra, R.; Walsh, R. *Chem. Rev.* **1995**, 95, 1203. (e) Walsh, R. In *The Chemistry of Organic*

*Silicon Compounds*; Patai, S., Rappoport, Z., Eds.; Wiley and Sons: Chichester, United Kingdom, 1989; Chapter 2, p 371.

(2) (a) Apeloig, Y. In *The Chemistry of Organic Silicon Compounds*; Patai, S., Rappoport, Z., Eds.; Wiley and Sons: Chichester, United Kingdom, 1989; Chapter 2, p 57. (b) Apeloig, Y. *Stud. Org. Chem.* **1987**, *31*, 33. (c) Apeloig, Y.; Merin-Aharoni, O. *Croat. Chem. Acta* **1992**, *65*, 757. (d) Lambert, J. B.; Kania, L.; Zhang, S. *Chem. Rev.* **1995**, *95*, 1191. (e) For a discussion of gas phase properties of silicenium ions, see: Acwarz, H. In *The Chemistry of Organic Silicon Compounds*; Patai, S., Rappoport, Z., Eds.; Wiley and Sons: Chichester, United Kingdom, 1989; Chapter 7, Vol. 1.

(3) Corriu, R. J. P.; Henner, M. *J. Organomet. Chem.* **1974**, *74*, 1.

(4) Eaborn, C. In *Organosilicon and Bioorganosilicon Chemistry*; Sakurai, H., Ed.; Ellis Horwood: Hemel Hempstead, United Kingdom, 1985.

(5) Olah, G. A.; Heiliger, L.; Li, X.-Y.; Prakash, G. K. S. *J. Am. Chem. Soc.* **1990**, *112*, 5991.

(6) Lickiss, P. D. *J. Chem. Soc., Dalton Trans.* **1992**, 1333.

(7) Prakash, G. K. S.; Keyaniyan, S.; Aniszfeld, R.; Heiliger, L.; Olah, G. A.; Stevens, R. C.; Choi, H.-K.; Bau, R. *J. Am. Chem. Soc.* **1987**, *109*, 5123.

(8) (a) Gomes de Mesquita, A. H.; MacGillavry, C. H.; Eriks, K. *Acta Crystallogr.* **1965**, *18*, 437. (b) Olah, G. A. *Top. Curr. Chem.* **1979**, *80*, 19.

(9) Apeloig, Y.; Stanger, A. *J. Am. Chem. Soc.* **1987**, *109*, 272.

(10) Xie, Z.; Liston, D. J.; Jelinek, T.; Mitro, V.; Bau, R.; Reed, C. A. *J. Chem. Soc., Chem. Commun.* **1993**, 384.

(11) (a) Lambert, J. B.; McConnell, J. A.; Schulz, W. J., Jr. *J. Am. Chem. Soc.* **1986**, *108*, 2482. (b) Lambert, J. B.; Schilf, W. *J. Am. Chem. Soc.* **1988**, *110*, 6364. (c) Lambert, J. B.; Schulz, W. J., Jr.; McConnell, J. A.; Schilf, W. *J. Am. Chem. Soc.* **1988**, *110*, 2201. (d) Lambert, J. B.; McConnell, J. A.; Schilf, W.; Schulz, W. J., Jr. *J. Chem. Soc., Chem. Commun.* **1988**, 455. (e) Lambert, J. B. In *The Chemistry of Organic Silicon Compounds*; Patai, S., Rappoport, Z., Eds.; Wiley and Sons: Chichester, United Kingdom, 1989; Chapter 16. (f) Lambert, J. B.; Kania, L.; Schilf, W.; McConnell, J. A. *Organometallics* **1991**, *10*, 2578. (g) Lambert, J. B.; Zhang, S.; Ciro, S. M. *Organometallics* **1994**, *13*, 2430.

(12) Eaborn, C. *J. Organomet. Chem.* **1991**, *405*, 173.

(13) Kira, M.; Hino, T.; Sakurai, H. *J. Am. Chem. Soc.* **1992**, *114*, 6697.

(14) Olah, G. A.; Rasul, G.; Heiliger, L.; Bausch, J.; Prakash, G. K. S. *J. Am. Chem. Soc.* **1992**, *114*, 7737.

(15) Reed, C. A.; Xie, Z.; Bau, R.; Benezi, A. *Science* **1993**, *262*, 402.

(16) Schleyer, P. v. R.; Buzek, P.; Müller, T.; Apeloig, Y.; Siehl, H.-U. *Angew. Chem., Int. Ed. Engl.* **1993**, *32*, 1471.

(17) (a) Lambert, J. B.; Zhang, S.; Stern, C. L.; Huffman, J. C. *Science* **1993**, *260*, 1917. (b) See also the debate between: Pauling, L.; Olah, G. A.; Rasul, G.; Li, X.-Y.; Buchholz, H. A.; Sandford, G.; Prakash, G. K. S.; Lambert, J. B.; Zhang, S. *Science* **1994**, *263*, 983.

(18) (a) Hiberty, P. C.; Flament, J. P.; Noizet, E. *Chem. Phys. Lett.* **1992**, *189*, 259. (b) Hiberty, P. C.; Humbel, S.; Byrman, C. P.; van Lenthe, J. H. *J. Chem. Phys.* **1994**, *101*, 5969.

(19) Hiberty, P. C.; Humbel, S.; Archirel, P. *J. Phys. Chem.* **1994**, *98*, 11697.

(20) Verbeek, J.; Langenberg, J. H.; Byrman, C. P.; van Lenthe, J. H. *TURTLE—An ab initio VB/VBSCF/VBCI program*; Theoretical Chemistry Group, Debye Institute, University of Utrecht, 1993.

(21) (a) Grein, F.; Chang, T. C. *Chem. Phys. Lett.* **1971**, *12*, 44. (b) Banerjee, A.; Grein, F. *Int. J. Quantum Chem.* **1976**, *10*, 123.

(22) Levy, B.; Berthier, G. *Int. J. Quantum Chem.* **1968**, *2*, 307.

(23) (a) Hunt, W. J.; Hay, P. J.; Goddard, W. A., III *J. Chem. Phys.* **1972**, *57*, 738. (b) Goddard, W. A.; Harding, L. B. *Annu. Rev. Phys. Chem.* **1978**, *29*, 363. (c) Bobrowicz, F. B.; Goddard, W. A. In *Methods of Electronic Structure Theory*; Schaefer, H. F., Ed.; Plenum Press: New York, 1977; pp 79–127.

(24) Davidson, E. R. *Chem. Phys. Lett.* **1973**, *21*, 565.

(25) Oberhammer, H.; Boggs, J. E. *J. Am. Chem. Soc.* **1980**, *102*, 7241.

(26) Chirgwin, B. H.; Coulson, C. A. *Proc. R. Soc. London, Ser. A* **1950**, *201*, 196.

(27) Weinhold, F.; Carpenter, J. *The Structure of Small Molecules and Ions*; Plenum Press: New York, 1988; p 227.

(28) Frisch, M. J.; Trucks, G. W.; Head-Gordon, M.; Gill, P. M. W.; Wong, M. W.; Foresman, J. B.; Johnson, B. G.; Schlegel, H. B.; Robb, M. A.; Replogle, E. S.; Gomperts, R.; Andres, J. L.; Raghavachari, K.; Binkley, J. S.; Gonzalez, C.; Martin, R. L.; Fox, D. J.; Defrees, D. J.; Baker, J.; Stewart, J. J. P.; Pople, J. A. *Gaussian 92, Revision C3*; Gaussian, Inc.: Pittsburgh PA, 1992.

(29) (a) Pople, J. A.; Head-Gordon, M.; Fox, D. J.; Raghavachari, K.; Curtis, L. A. *J. Chem. Phys.* **1989**, *90*, 5622. (b) Curtis, L. A.; Raghavachari, K.; Trucks, G.; Pople, J. A. *J. Chem. Phys.* **1991**, *94*, 7221.

(30) For H<sub>3</sub>C–Cl, see: *J. Phys. Chem. Ref. Data* **1974**, *3*, 392. For H<sub>3</sub>Si–Cl, see: *J. Phys. Chem. Ref. Data* **1982**, *11*, 745.

(31) Shaik, S. In *New Concepts for Understanding Organic Reactions*; Bertran, J., Csizmadia, I. G., Eds.; NATO ASI Series; Kluwer: Dordrecht, 1989; Vol. C267.

(32) (a) Shaik, S.; Maître, P.; Sini, G.; Hiberty, P. C. *J. Am. Chem. Soc.* **1992**, *114*, 7861. (b) Sini, G.; Maître, P.; Hiberty, P. C.; Shaik, S. *J. Mol. Struct. (THEOCHEM)* **1991**, *229*, 163.

(33) (a) Sini, G. Ph.D. Thesis, Université de Paris-Sud, Orsay, France, 1990: A VB calculation of (FSiH<sub>3</sub>F)<sup>−</sup> shows that the lowest VB structure is X<sup>−</sup>R<sub>3</sub>Si<sup>+</sup>X<sup>−</sup>, and its resonance energy due to mixing with the covalent structures is ca. 65 kcal/mol. (b) For a discussion of (FSiH<sub>3</sub>F)<sup>−</sup>, see: Shaik, S.; Hiberty, P. C. *Adv. Chem. Phys.* **1995**, *26*, 99–163.

(34) Gronet, S.; Glaser, R.; Streitwieser, A. *J. Am. Chem. Soc.* **1989**, *111*, 3111.

(35) For a variety of R<sub>3</sub>C<sup>+</sup>X<sup>−</sup> solids, see: Laube, T. *Acc. Chem. Res.* **1995**, *28*, 399.

JP960145L